



Preliminary Study of the $\text{La}_{4-x}\text{A}_x\text{Ni}_3\text{O}_{10-\delta}$ (A = Na, K and Sr) Systems as IT-SOFC Cathode Materials (U)

D. Au
University of Waterloo

G. Amow
DRDC Atlantic

Defence R&D Canada – Atlantic

Technical Memorandum
DRDC Atlantic TM 2008-218
May 2009

This page intentionally left blank.

Preliminary Study of the $\text{La}_{4-x}\text{A}_x\text{Ni}_3\text{O}_{10-\delta}$ (A = Na, K and Sr) Systems as IT-SOFC Cathode Materials (U)

D. Au
University of Waterloo

G. Amow
DRDC Atlantic

Defence R&D Canada – Atlantic

Technical Memorandum
DRDC Atlantic TM 2008-218
May 2009

Principal Author

Original signed by G. Amow

G. Amow

Defence Scientist/Air Vehicle Research Section

Approved by

Original signed by K. McRae

Mr. Ken McRae

Head/Air Vehicle Research Section

Approved for release by

Original signed by Ron Kuwahara for

Calvin Hyatt

Chair Document Review Panel/DRDC Atlantic

- © Her Majesty the Queen in Right of Canada, as represented by the Minister of National Defence, 2009
© Sa Majesté la Reine (en droit du Canada), telle que représentée par le ministre de la Défense nationale, 2009

Abstract

A preliminary study of the $\text{La}_{4-x}\text{A}_x\text{Ni}_3\text{O}_{10-\delta}$ ($\text{A} = \text{Na}, \text{K}$ and Sr) system was carried out to determine their viability as IT-SOFC cathodes. For this study, two synthesis routes were used, both of which showed limited solubility ranges of the A-site doped cations. Physical property measurements show an enhancement of the electrical conductivity with A-site cation doping, good thermal stability and thermal expansion coefficients of $\alpha \sim 12.90 - 13.05 \times 10^{-6} \text{ K}^{-1}$. Scanning electron microscopy demonstrated significant differences in the particulate morphologies resulting from the different synthetic routes, which helps to explain the relatively rapid synthesis times of the glycine-nitrate process versus Pechini method.

Résumé

On a réalisé une étude préliminaire portant sur les matériaux de compositions $\text{La}_{4-x}\text{A}_x\text{Ni}_3\text{O}_{10-\delta}$ (où $\text{A} = \text{Na}, \text{K}$ et Sr) afin de déterminer leur efficacité comme cathodes de piles à combustible à oxyde solide à température intermédiaire (IT-SOFC). Dans le cadre de la présente étude, on a utilisé deux procédés de synthèse dont les résultats indiquent que les cations dopés présents en position A présentent, dans les deux cas, des plages restreintes de solubilité. Les mesures de certaines propriétés physiques mettent en évidence l'augmentation de la conductivité électrique découlant du dopage du cation présent en position A, ainsi qu'une bonne stabilité thermique et un coefficient de dilatation thermique (α) se situant dans la plage approximative de 12,90 à 13,05 $\times 10^{-6} \text{ K}^{-1}$. L'analyse des matériaux par microscopie électronique à balayage démontre que les morphologies des particules présentent des différences notables, attribuables à la nature des procédés de synthèse, ce qui permet d'expliquer les vitesses de synthèse relativement élevées propres au procédé glycine-nitrate, comparativement à la méthode Pechini.

This page intentionally left blank. Cette page est intentionnellement laissée en blanc.

Executive summary

Preliminary Study of the $\text{La}_{4-x}\text{A}_x\text{Ni}_3\text{O}_{10-\delta}$ (A = Na, K and Sr) Systems as IT-SOFC Cathode Materials (U):

D. Au and G. Amow; DRDC Atlantic TM 2008-218; Defence R&D Canada – Atlantic; May 2009.

Introduction or background: Solid-oxide fuel cells are electrochemical devices, which convert the chemical energy stored in a fuel into usable electrical power. They require relatively high temperatures for operation and as a result of this, can suffer long-term thermal degradation and thermal expansion incompatibility issues within the cell component materials such as the cathode, anode and electrolyte. To mitigate these problems, it is essential to lower the operating temperature of the fuel cell stack (~650°C-800°C) and in doing so, it is necessary to discover new materials with optimized performance for the cell components in this intermediate temperature range.

Results: A series of novel cathode materials were prepared and characterized for intermediate-temperature solid oxide cathode-use based on the Ruddlesden-Popper materials $\text{La}_{4-x}\text{A}_x\text{Ni}_3\text{O}_{10}$ (A = Na, Sr, K). Through systematic substitution of these cations on the A-site, improvements in both the electrical conductivity and thermal expansion coefficients were observed.

Significance: With the increasing demands of power and energy in the Canadian Forces, it is of paramount importance to discover solutions, which meet these requirements. In particular, the Canadian Forces of tomorrow require advanced power systems that are efficient, quiet and deliver high energy densities, which will allow for longer mission times and cost-benefits. Solid-oxide fuel cells are of particular interest for military-use due to its high-temperature operation (900°C-1000°C), which allows fuel flexibility and cogeneration benefits.

Future plans: Further work is planned on optimizing these materials for solid-oxide fuel cell cathode-use, which includes doping studies with other A-site ions e.g. neodymium and electrochemical characterization by area specific resistance and single-cell measurements under hydrogen.

Sommaire

Étude préliminaire de matériaux de compositions $\text{La}_{4-x}\text{A}_x\text{Ni}_3\text{O}_{10-\delta}$ (où A = Na, K et Sr) pouvant servir de cathodes de piles à combustible du type IT-SOFC :

D. Au et G. Amow; RDDC Atlantique TM 2008-218; R & D pour la défense Canada – Atlantique; mai 2009.

Introduction : Les piles à combustible à oxyde solide constituent des dispositifs électrochimiques ayant la capacité de transformer l'énergie chimique inhérente d'un combustible en énergie électrique utilisable. Leur fonctionnement adéquat requiert des températures relativement élevées et, conséquemment, elles peuvent subir une dégradation thermique à long terme et présenter des problèmes d'incompatibilité au chapitre des différents coefficients de dilatation thermique des matériaux qui les composent, par exemple la cathode, l'anode et l'électrolyte. Afin d'atténuer l'importance de ces problèmes, il est essentiel d'abaisser l'intervalle de températures de fonctionnement de la pile à combustible (environ 650 à 800 °C), et il faut donc mettre au point de nouveaux matériaux pouvant être utilisés pour fabriquer des composants de la pile et présentant un rendement optimal dans la plage de températures intermédiaires susmentionnée.

Résultats : On a préparé et caractérisé une série de nouveaux matériaux pouvant servir de cathodes de piles à combustible à oxyde solide à température intermédiaire (IT-SOFC); la composition des matériaux préparés est basée sur celle de matériaux du type Ruddlesden-Popper, soit $\text{La}_{4-x}\text{A}_x\text{Ni}_3\text{O}_{10}$ (où A = Na, Sr, K). En effectuant une substitution systématique des ces trois cations en position A, on observe une amélioration des capacités en matière de conductivité électrique et de coefficients de dilatation thermique.

Portée : Les Forces canadiennes ont des besoins croissants au chapitre des sources d'énergie et il est donc essentiel de trouver des solutions qui permettent de répondre à ces besoins particuliers. Les Forces canadiennes de demain auront notamment besoin de dispositifs d'alimentation de pointe efficaces et très peu bruyants, qui ont la capacité d'offrir une densité d'énergie élevée et permettent ainsi d'accroître la durée des missions et d'optimiser le rapport coûts-avantages. Les piles à combustible à oxyde solide présentent un intérêt particulier en ce qui a trait aux applications militaires, grâce, notamment aux températures de fonctionnement élevées qui leur sont propres (de 900 à 1000 °C), ce qui permet d'employer divers combustibles et présente des avantages en matière de cogénération.

Recherches futures : On prévoit exécuter des travaux supplémentaires visant à optimiser les propriétés de ces matériaux utilisés comme cathodes de piles à combustible à oxyde solide, notamment des études sur le dopage d'autres ions présents en position A (par exemple, le néodyme), ainsi que la caractérisation électrochimique par résistivité et des mesures de rendement d'une pile sous atmosphère d'hydrogène.

Table of Contents

Abstract	i
Executive summary	iii
Sommaire.	iv
Table of Contents	v
List of figures	vi
List of tables	vii
Acknowledgements	viii
1 Introduction.....	1
2 Experimental Procedure.....	4
2.1 Pechini Synthesis.....	4
2.2 Glycine-Nitrate Process (GNP)	5
2.3 X-ray Diffraction	5
2.4 Oxygen Content Determination.....	6
2.5 d.c. Electrical Conductivity	6
2.6 Thermomechanical Analysis (TMA).....	6
2.7 Long-Term Stability Tests.....	7
2.8 Scanning Electron Microscopy (SEM).....	7
3 Results and Discussion	8
3.1 Observations of the Pechini Synthesis.....	8
3.2 Observations of the GNP Synthesis.....	9
3.3 Scanning Electron Microscopy (SEM).....	10
3.4 Cell Constants and Oxygen Contents	12
3.5 Electrical Conductivity	13
3.6 Thermomechanical Analysis	14
3.7 Long-Term Thermal Stability.....	14
4 Summary and Conclusions	16
5 References	17
Distribution list	19

List of figures

Figure 1: Schematic diagram of a solid-oxide fuel cell [2]	1
Figure 2: Crystal Structure of the Ruddlesden-Popper phases	2
Figure 3: Pechini synthesis of $\text{La}_{4-x}\text{Sr}_x\text{Ni}_3\text{O}_{10\pm\delta}$ ($x = 0.1 - 0.5$); $\text{La}_2\text{NiO}_{4+\delta}$ impurity (*).	9
Figure 4: XRD patterns of the raw precursors obtained from the GNP method with different glycine:metal ion ratios.	11
Figure 5: SEM images of Pechini (left) and GNP (right) $\text{La}_{3.9}\text{Sr}_{0.1}\text{Ni}_3\text{O}_{10}$ raw precursors.....	11
Figure 6: Electrical Conductivity of phase pure $\text{La}_{4-x}\text{A}_x\text{Ni}_3\text{O}_{10}$ samples.....	13
Figure 7: Thermomechanical Analysis of $\text{La}_{4-x}\text{A}_x\text{Ni}_3\text{O}_{10}$ and undoped $\text{La}_4\text{Ni}_3\text{O}_{10}$	15

List of tables

Table 1: Cell Constants and Delta Values of Single Phase Compositions	12
Table 2: Densities of Single Phase Compositions	14
Table 3: Thermal Expansion Coefficients of Single Phase Compositions	15

Acknowledgements

The authors thank Mr. Dave Kingston from the National Research Council for his assistance with the scanning electron microscopy measurements.

1 Introduction

Solid-oxide fuel cells (SOFCs) offer promise as an alternative source of energy, which can be utilized in stationary and portable power applications. First generation SOFCs operate at high temperatures ($\sim 1000^{\circ}\text{C}$). However, due to these high temperatures, the component materials of the stack suffer thermal and chemical degradation due to incompatibilities with other cell components. Current research trends target an intermediate temperature range for operation defined as $\sim 650^{\circ}\text{C}$ - 800°C , which is expected to lower degradation rates and result in reduced operating costs. However, with decreased operating temperature comes a decrease in the performance of the conventional materials, thus underscoring the need for discovering new materials. [1]

Similar to many other types of fuel cells, SOFCs consist mainly of a cathode, electrolyte, and an anode. In order to generate an electric current, air is passed through the cathode where oxygen is reduced to form oxygen ions. Hydrogen fuel is passed through the anode and oxygen ions pass through the electrolyte to oxidize at the anode to form water and electrons, which can be used to power a device as shown in Figure 1.

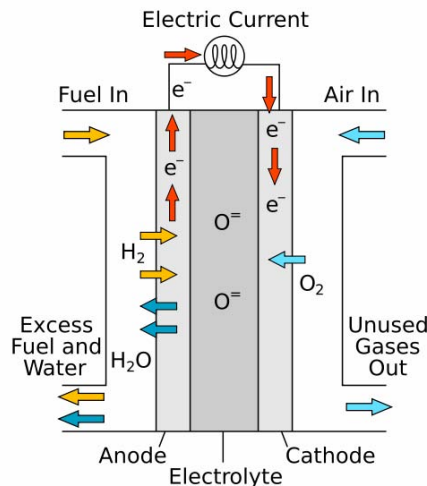


Figure 1: Schematic diagram of a solid-oxide fuel cell [2]

Since the largest polarization losses originate from the cathode, improving the properties of the cathode is essential for long-term use. Desired characteristics of interest for the cathode

are significant electrical and ionic conductivity, compatible thermal expansion coefficients with other cell components, as well as long-term thermal stability. [1,2]

Traditional cathode materials are based on the perovskite structure, which possesses good electronic and ionic conductivity at high temperatures. However, at high temperatures these materials degrade thermally and chemically leading to the subsequent breakdown of the cell. Of interest have been Ruddlesden-Popper materials, $R_{n+1}M_nO_{3n+1}$. In particular, the Ruddlesden-Popper $n = 1$ phase, $La_2NiO_{4+\delta}$, has been the source of much interest due to the enhanced oxide ionic conductivity compared to the traditional perovskite materials [3]. This is a consequence of its crystallographic structure as seen in Figure 2, which comprises of alternating perovskite and rock salt layers. Such a structure has a higher degree of interstitial sites on which additional oxide ions can reside thus influencing the oxygen-ion diffusion mechanism. This particular material, however, does not have good long-term stability and the higher order $n = 3$ phase, $La_4Ni_3O_{10-\delta}$, was found to be more promising as an ITSOFC cathode. [3,4]

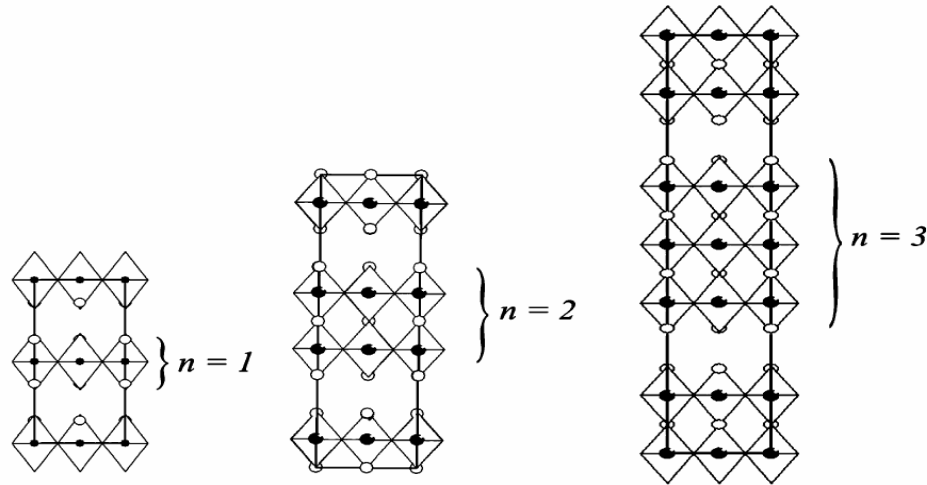


Figure 2: Crystal Structure of the Ruddlesden-Popper phases

To further improve the characteristics of the Ruddlesden-Popper $n = 3$ material, studies with various B-site dopants, $La_4Ni_{3-x}B_xO_{10-\delta}$, such as cobalt, copper and iron at the B-site have been undertaken. In short summary, it was found that cobalt doping resulted in lower electric conductivity, poor stability and poor thermal expansion coefficients [4]; doping with copper resulted in significantly improved electrical conductivity [5] while iron doping resulted in

reduced electrical conductivity with a slight decrease in the thermal expansion coefficients with increased doping [6]. The present study is focused on A-site doping with strontium, potassium and sodium, $\text{La}_{4-x}\text{A}_x\text{Ni}_3\text{O}_{10-\delta}$. Due to the differences in the ionic radii of strontium, potassium and sodium as well as being monovalent cations, it is of interest to determine the effect of cation size and the relative $\text{Ni}^{2+}/\text{Ni}^{3+}$ content on the physical properties.

In our previous studies, the Pechini method [7] was routinely used for materials synthesis. For the present study, the Glycine-Nitrate Process synthesis (GNP) [8] was also investigated to reduce synthesis times as well as obtaining smaller particle morphologies.

2 Experimental Procedure

2.1 Pechini Synthesis

In the typical Pechini method, stoichiometric amounts of metal nitrates are dissolved in water to which have been added calculated amounts of citric acid and ethylene glycol. This mixture is then heated on a hot plate to decompose the nitrates and promote the eventual formation of the polymeric precursor, which is then subsequently treated to derive the desired products. However, the process required modification due to the relatively high melting point of $\text{Sr}(\text{NO}_3)_2$, which is not easily decomposed on the hotplate. In the modified process, half of the required amount of citric acid and ethylene glycol is added. Concentrated ammonium hydroxide was then added dropwise in order to help dissociate the strontium nitrate, which immediately formed a greenish thick precipitate $[\text{Ni}(\text{OH}_2)]$ in a deep blue solution between pH 2 and 8. More ammonium hydroxide was added until the precipitate was eventually dissolved at ~ between pH 8-9 after which no more hydroxide was added. Note that this addition was done while no heat was added to the beaker. It was determined that a citric acid (CA) to ethylene glycol (EG) ratio of 3:1 was necessary to form single phase $x = 0.1$ strontium composition as it prevented the formation of the $\text{La}_2\text{NiO}_{4+\delta}$ impurity phase when other ratios were used. It was also noted that during this procedure, the manner in which the CA and EG was added was important; only half the required amount was added at the beginning. At pH 9, when the solutions were deep blue in colour with no precipitate, heat was applied to the beaker. During the evaporation process, the greenish thick precipitate reformed at ~ pH 7.5. At this point, it was essential to redissolve this precipitate by adding ~35mL more concentrated ammonium hydroxide followed by the addition of the remaining half of the required amount of CA and ethylene glycol. This prevented further precipitate formation as the lower pH values were obtained on evaporation. Once the solution was evaporated and the polymeric residue was formed, it was placed in the drying oven overnight at ~ 120°C, which produced a thick and tar-like black residue. This residue was ground in an agate mortar and set to fire in the furnace in several temperature steps: 200°C, 400°C, 750°C and eventually at 1000°C. Doing these stepwise firings were necessary to minimize

contamination of the furnace due to the combustion ammonium nitrate now present in the samples; the samples were placed into a glass evaporating dish with an inverted glass dish and the sides plugged with high-temperature resistant fire blanket. The procedure described here was used to prepare phases of $\text{La}_{4-x}\text{Sr}_x\text{Ni}_3\text{O}_{10\pm\delta}$ where $x = 0.1, 0.2, 0.3, 0.4,$ and 0.5 .

2.2 Glycine-Nitrate Process (GNP)

As in the Pechini synthesis, stoichiometric amounts of each metal nitrate required to form the desired mass of product was weighed out and dissolved in distilled water in a 2L stainless steel beaker, which was covered with a stainless steel mesh to prevent escape of the particles on combustion. It was found that the optimum glycine to metal-nitrate ratio 2:1 was for final product formation (other ratios were used such as 6:1, 3:1 and 1.5:1 with no success). On heating and subsequent evaporation, the contents of the beaker self-combusted in a violent manner. The resulting raw precursor, black in colour, was ground up, pressed into pellets and fired at 1000°C . Depending on phase purity, the product would be reground, repressed and fired again at 1000°C . The GNP synthesis was used to produce $\text{La}_{4-x}\text{Sr}_x\text{Ni}_3\text{O}_{10-\delta}$, $\text{La}_{4-x}\text{K}_x\text{Ni}_3\text{O}_{10-\delta}$, $\text{La}_{4-x}\text{Na}_x\text{Ni}_3\text{O}_{10-\delta}$ where $x = 0.05, 0.10, 0.15, 0.20,$ and 0.30 .

2.3 X-ray Diffraction

XRD was performed with a D8 x-ray diffractometer with $\text{CuK}\alpha_1$ after each firing to determine phase purity and the scanning parameters for the short scans were $2\theta = 10^\circ - 80^\circ$ with steps of 0.04° and a step count of 2 seconds. Phase purity was determined by comparing the short scans to the patterns in the JC-PDF database using Diffrac Plus Evaluation Eva software. XRD was also used to determine cell constants from long scans with data collected at $2\theta = 10^\circ - 100^\circ$ with steps of 0.02° and a step count of 10 seconds. The cell constants were calculated least squares fitting with the software *TOPAS*.

2.4 Oxygen Content Determination

Oxygen content determination was performed with potentiometric iodometric titration using a Metrohm Autotitrator GPD Titrino 751. In this titration, sodium thiosulphate was used to reduce iodide ions where the amount of iodine formed in solution depended on the amount of dissolved sample. The amount of thiosulphate used for titrating was used to calculate the oxygen content of the sample.

2.5 d.c. Electrical Conductivity

To prepare the samples for electrical conductivity measurements by the van der Pauw (VDP) method, a 12mm x 12mm square die was used to press pellets of ~1-2mm thickness. These square pellets were fired at 1000°C and placed on the VPD sample holder. An in-house Labview program controlling a Thermolyne 21100 Tube Furnace, Barnant Company Temperature Controller R/S, Keithley 2400 Source Meter and a 2700 Multimeter/data acquisition system was used to perform the conductivity measurements.

2.6 Thermomechanical Analysis (TMA)

The samples for TMA were cut from a circular pellet using an Isomet 11-1180 Low Speed Saw with a 15 LC Buehler diamond wafering blade to yield a rectangular bar with dimensions of ~2mm x ~2 mm x ~12mm. For cutting, the sample was glued onto a cutting block hot wax, and after being cut, the sample was removed with acetone to dissolve the wax. A TA Instruments TMA 2940 measured the length changes of a sample over a temperature range of 25°C to 900°C with an applied downward force of 0.250N. A blank run was performed first to account for the expansion of the stage and probe before the samples were loaded onto the stage. All runs were done in static air.

2.7 Long-Term Stability Tests

Pressed pellets of $x = 0.15$ Sr, $x = 0.20$ Na and K and potassium (12mm diameter) were fired at 1000°C for two weeks. The samples were analyzed after this process with XRD to verify any impurity formation.

2.8 Scanning Electron Microscopy (SEM)

A JEOL 840A scanning electron microscope equipped with an Oxford Instruments 6560 INCAx-sight light element energy dispersive x-ray (EDX) spectrometer was used to explore the morphological difference between the Pechini and GNP synthesis routes. The spectrometer consists of a super atmospheric thin window and Si (Li) crystal that detects Beryllium to Uranium and has a spectral resolution of 129eV. The spectra were collected with a total live time of 60s and all photos were scanned using an accelerating voltage of 20kV with a working distance of 15mm.

3 Results and Discussion

3.1 Observations of the Pechini Synthesis

After the nitrates were dissolved in solution, the solution had a transparent bright green colour due to the nickel content. When the water was evaporating, the solution became more viscous and as it dried up, a dry brown resin was formed, which became darker brown after placing the precursor in the vacuum oven overnight at 180°C. After the 400°C firing, the material remained at a dark brown colour eventually turning to dark grey and then black after the 750°C and 1000°C firings respectively.

When doping with strontium, a CA/EG:metal nitrates ratio of 1.5:1 was used but a precipitate formed throughout the water evaporation process; this precipitate was found to be nickel hydroxide and the source may have been incomplete chelation of the metal ions. Therefore, a greater ratio of 3:1 was used and the CA and EG were added to the solution in two separate steps; half of the theoretical amount of CA and EG before adding the ammonium hydroxide and half after. This was observed from the XRD scans to yield a higher purity.

Of all the samples synthesized using the Pechini synthesis, only $\text{La}_{4-x}\text{Sr}_x\text{Ni}_3\text{O}_{10\pm\delta}$ where $x = 0.1$ was found to be single phase. The $x = 0.2, 0.3, 0.4,$ and 0.5 compositions contained the La_2NiO_4 impurity in systematically increasing amounts as seen in Figure 3. From this data, it was thought that the solubility limit of strontium may have been reached due to its ionic radii or perhaps that the modified Pechini synthesis method was not optimized, which consequently lead to utilizing the GNP method.

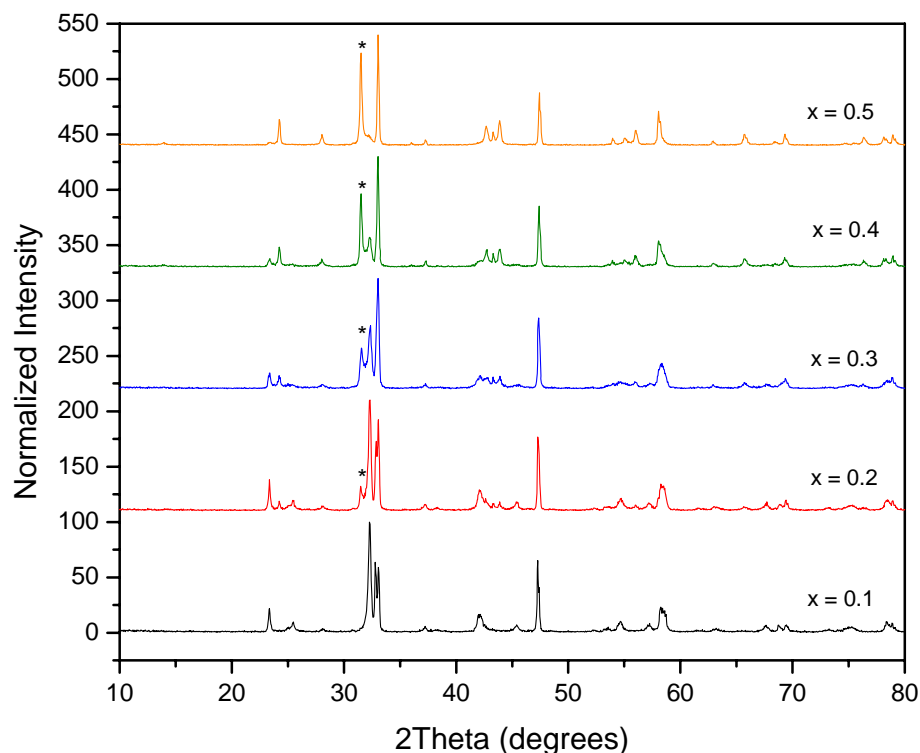


Figure 3: Pechini synthesis of $\text{La}_{4-x}\text{Sr}_x\text{Ni}_3\text{O}_{10\pm\delta}$ ($x = 0.1 - 0.5$); $\text{La}_2\text{NiO}_{4\pm\delta}$ impurity (*).

3.2 Observations of the GNP Synthesis

Solutions were transparent light green in colour after dissolving in water. On heating and subsequent evaporation, the self-combustion reaction occurred, which was rapid (~1-2 seconds) to produce very fine powders. During the reactions, flames sometimes reached out of the beaker with the expulsion of particles from the beaker. To minimize significant loss of product, a metal mesh was used to cover the top of the beaker as well as to reduce flame height. Several experiments were carried out to determine the optimum glycine to metal ion ratios for phase-pure product. These were 6:1, 3:1, 2:1 and 1.5:1. XRD patterns of the raw precursors obtained from these ratios after self-combustion are shown in Figure 4. Based on the very broad peaks obtained when the 6:1 and 3:1 ratios were used, it was evident that the

reaction temperature was too low. Subsequent firing at 1000°C, produced the La₂NiO₄ impurity, which when formed is very difficult to remove. This suggested that a reduction reaction was taking place due to the relatively high organic residue in the precursors. The impurity phase was also formed when a ratio of 1:1 was used. This, however, was not due to having high amounts of organic residue but instead likely due to the much higher combustion temperatures in the beaker. Consequently, it was found that a ratio of 2:1 was crucial in forming single phase product. The XRD pattern of the 2:1 precursor shows the presence of well-defined peaks of La₂O₃ and NiO with very little organic residue. On reacting at 1000°C for 6 hours, several single-phases were attained. Compositions synthesized with GNP that attained single phase purity were La_{4-x}A_xNi₃O_{10±δ} where $x \leq 0.15$ for strontium and potassium, and $x \leq 0.10$ for sodium as a small NiO impurity was noted for higher contents. Since single phases were not obtained for the higher content strontium doped samples, it was confirmed that the solubility limit was not due to limitations by the modified Pechini synthesis technique but instead due to the cation sizes of the dopants. Nevertheless, the GNP method provides a quick route to product with fewer steps in significantly less time; at least five process steps and five days were required to produce single-phase product by the Pechini method whereas only two process steps and two days were used in the GNP method.

3.3 Scanning Electron Microscopy (SEM)

Scanning Electron Microscopy was used to compare the particle size and morphologies of the raw precursors attained from the Pechini and GNP methods. The samples compared were raw precursors of Pechini (sample after firing at 750°C; DA01-89) and GNP (sample right after self-combustion reaction; DA01-139CS). The SEM images show particulates formed from the GNP synthesis are sponge-like with many tunnels yielding high porosity an surface area while the Pechini sample still had strands of organic material. The higher surface area in the former explains readily the rapid formation of product on heating to 1000°C in air.

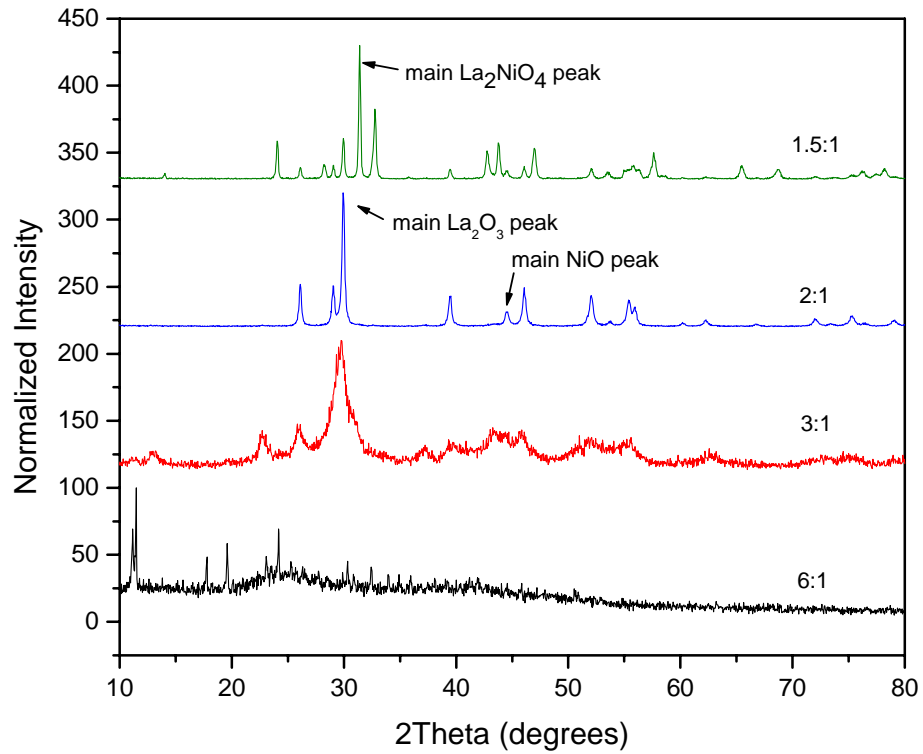


Figure 4: XRD patterns of the raw precursors obtained from the GNP method with different glycine:metal ion ratios.

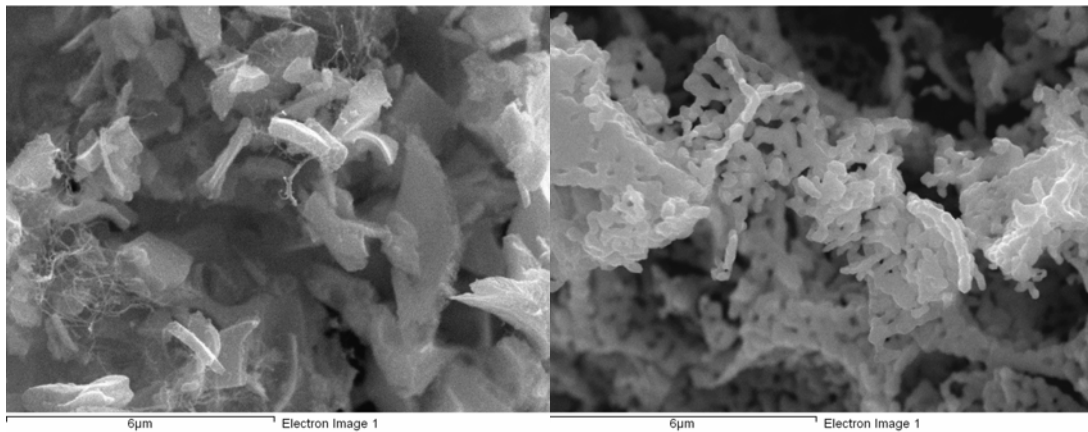


Figure 5: SEM images of Pechini (left) and GNP (right) $\text{La}_{3.9}\text{Sr}_{0.1}\text{Ni}_3\text{O}_{10}$ raw precursors

3.4 Cell Constants and Oxygen Contents

Table 3.1 summarizes the cell constants and oxygen contents (δ in $\text{La}_{4-x}\text{A}_x\text{Ni}_3\text{O}_{10\pm\delta}$) obtained for various compositions of doping with strontium, sodium and potassium. All materials synthesized are noted to be oxygen deficient, which suggests that the oxide-ion diffusion mechanism may occur via both oxide ion defects as well as the interstitial sites potentially leading to higher oxide-ion diffusion coefficients compared to the conventional cathode materials. As shown in the table, the ionic radii of the metal ions influence the cell constants and overall unit cell volume. In comparing the similar doping levels between the Na and K phases, the overall cell volume increases due to increasing cation size. Also noted is a slight decrease in the cell volume as x increases to 0.15 and is attributed to greater Ni^{3+} content present. These small changes suggests smaller bond angles, which lead to better electron orbital overlap and thus better electronic conductivity through decreased band gaps.

Table 1: Cell Constants and Delta Values of Single Phase Compositions

Sample – ionic radii [9]		a (Å)	B (Å)	C (Å)	V/Å ³	Delta (δ)
La - 1.36 Å		5.4622	5.4144	27.9748	827.34	-0.22
(pure)						
Sr – 1.44 Å	0.10	5.4591	5.4216	27.9980	828.6558	-0.05
	0.15	5.4623	5.4174	27.9670	827.5844	-0.08
Na – 1.39 Å	0.05	5.4632	5.4137	27.9546	826.7888	-0.14
	0.10	5.4636	5.4151	27.9444	826.7614	-0.16
K – 1.64 Å	0.05	5.4644	5.4149	27.9629	827.3992	-0.08
	0.10	5.4633	5.4140	27.9587	826.9710	-0.21

3.5 Electrical Conductivity

The electrical conductivity was determined by the Van der Pauw technique with the cooling data shown in Figure 6; only data of the samples which were single phase and whose cell constants were found are plotted. As seen in the above graph, doping with strontium does not improve conductivity in the intermediate temperature range until $x = 0.15$; however, doping with sodium and potassium yields more desirable results. The sodium $x = 0.10$ and potassium $x = 0.05$ samples show the best electrical conductivity in the intermediate temperature range. It is worth noting that the measured densities of the sample are similar as shown in Table 2. While the absolute conductivity values are high, they are underestimated due to the low pellet densities obtained for the measurements.

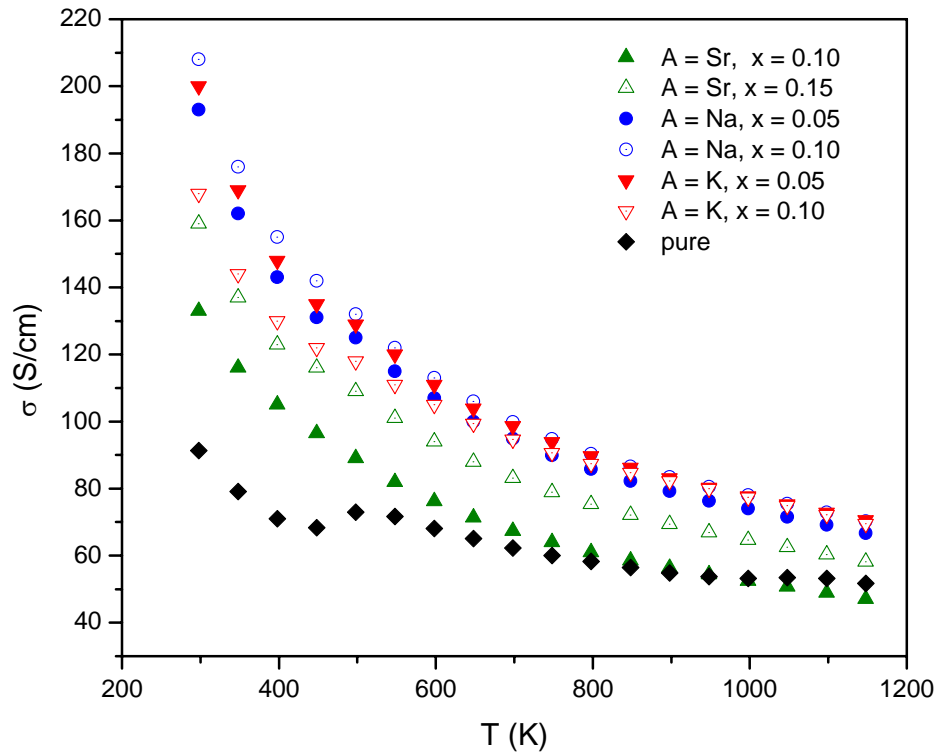


Figure 6: Electrical Conductivity of phase pure $\text{La}_{4-x}\text{A}_x\text{Ni}_3\text{O}_{10}$ samples

Table 2: Densities of Single Phase Compositions

Composition	x	theoretical density (g/cm ³)	experimental density (g/cm ³)	% density
Sr	0.10	7.106	3.095	43.6
	0.15	7.095	3.240	45.7
Na	0.05	7.117	3.284	46.1
	0.10	7.071	3.317	46.9
K	0.05	7.118	3.150	44.3
	0.10	6.609	3.421	51.8

3.6 Thermomechanical Analysis

Thermomechanical analysis (TMA) was used to determine the thermal expansion coefficients (TEC) of several single phase samples shown in Figure 7 and whose values are summarized in Table 3.3. From the table, observations can be made that all the samples have similar TECs and also do not differ from undoped La₄Ni₃O₁₀. These values are within 15% of LSGM-9182 (electrolyte), which is considered acceptable.

3.7 Long-Term Thermal Stability

The samples with compositions of x = 0.15 strontium, x = 0.20 sodium and potassium were fired in a furnace at 1000°C for two weeks in air. XRD scans of the samples show no

impurity formation of the La_2NiO_4 phase under these conditions and are stable.

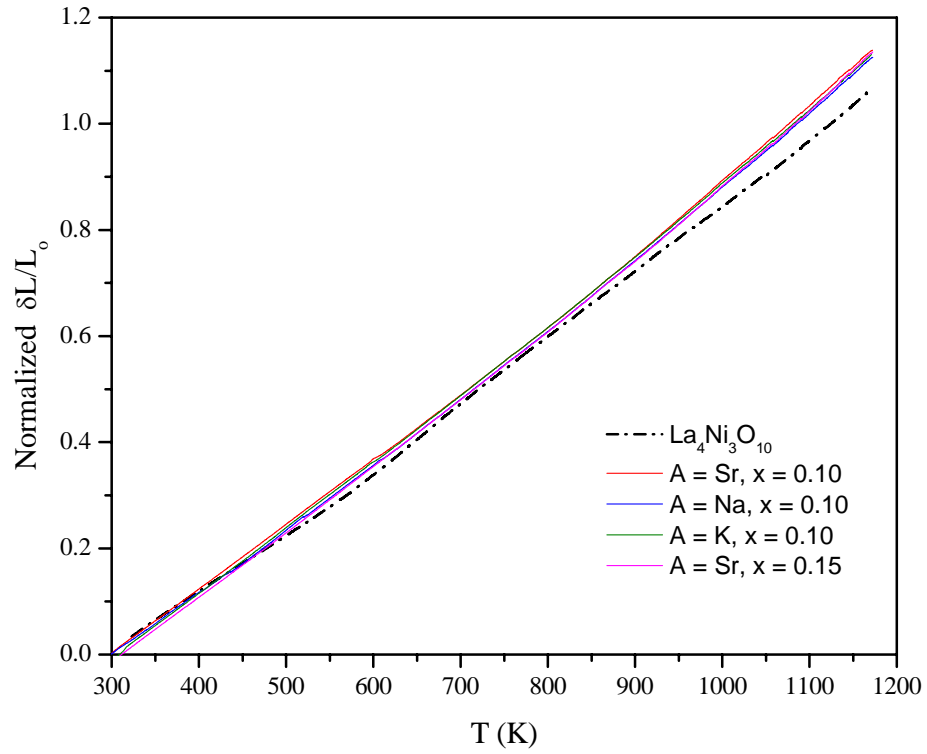


Figure 7: Thermomechanical Analysis of $\text{La}_{4-x}\text{A}_x\text{Ni}_3\text{O}_{10}$ and undoped $\text{La}_4\text{Ni}_3\text{O}_{10}$

Table 3: Thermal Expansion Coefficients of Single Phase Compositions

Composition	x	$\alpha \times 10^{-6} / ^\circ\text{C}$
Strontium	0.10	12.97
	0.15	13.05
Sodium	0.10	12.90
Potassium	0.10	13.00
Pure [3]	0	13.10
Electrolyte ($\text{La}_{0.9}\text{Sr}_{0.1}\text{Ga}_{0.8}\text{Mg}_{0.2}\text{O}_3$)	n/a	11.5

4 Summary and Conclusions

The A-site doped series $\text{La}_{4-x}\text{A}_x\text{Ni}_3\text{O}_{10}$ were prepared by two synthesis routes via a modified Pechini process and the GNP method; the latter method being very efficient with reduced synthesis steps and process times. Single phase materials of strontium $x \leq 0.15$, sodium $x \leq 0.10$ and potassium $x \leq 0.15$, were produced and characterized through XRD, iodometric titration, d.c. electrical conductivity, TMA and long-term stability tests. All materials were found to be oxygen deficient, which have implications for the oxide-ion diffusion mechanism and should be investigated further with ion-exchange depth profiling with isotopic oxygen. For electrical conductivity, the sodium and potassium doped samples show a significant improvement compared to the pure sample in the intermediate temperature range. The thermal expansion coefficients were within an acceptable range compared to the electrolyte LSGM-9182. As important, the long-term stability test revealed these materials to be thermally stable. These results suggest these materials to be viable candidates for IT-SOFC cathodes; however, further electrochemical characterization is required to confirm this.

5 References

- [1] S.C. Subhash and K.Kendall, *High Temperature Solid Oxide Fuel Cells*, Elsevier, 2003
- [2] C.K.M. Shaw, Mass Transport in Mixed Conduction Perovskite Related Oxides, PhD Thesis, Imperial College of Science, Technology and Medicine, 2001 p.65
- [3] G. Amow and S. J. Skinner, "Recent Developments in Ruddlesden-Popper Nickelate Systems for Solid Oxide Fuel Cell Cathodes", *J Solid State Electrochem*, January 2006, pp. 538-545
- [4] G. Amow, J. Au, and I. Davidson, "Synthesis and Characterization of $\text{La}_4\text{Ni}_{3-x}\text{Co}_x\text{O}_{10\pm\delta}$ ($0.0 \leq x \leq 3.0$, $\Delta x = 0.2$) for Solid Oxide Fuel Cell Cathodes", *Solid State Ionics*, 2006, pp. 177, 1837-1841
- [5] G. Amow and A. Parisien, "Evaluation of $\text{La}_4\text{Ni}_{3-x}\text{Cu}_x\text{O}_{10}$ Novel Materials for Solid-oxide Fuel Cell Cathodes", *Conference Proceedings of the 2007 CF/DRDC International Defence Applications of Materials Meeting*, Halifax, NS
- [6] Amow, G.; Parisien, A.; Chan, J. An Investigation of the Physical Properties of the $\text{La}_4\text{Ni}_{3-x}\text{B}_x\text{O}_{10-\delta}$ System (B = Cu, Fe) for Solid Oxide Fuel Cell Cathodes, Proceedings of the 8th EUROPEAN SOLID OXIDE FUEL CELL FORUM, Lucerne, Switzerland, June 30th-July 4th, 2008, Bossel, U., Ed. European Fuel Cell Forum: Lucerne, Switzerland, 2008; p A0614.
- [7] M. Pechini, "Method of Preparing Lead and Alkaline-Earth Titanates and Niobates and Coating Method Using the Same to Form a Capacitor", *U.S. Patent No. 3,330,697*, July 11, 1967
- [8] L.A. Chick, L.R. Pederson, G.D. Maupin, J.L. Bates, L.E. Thomas and G.J. Exarhos, "Glycine-nitrate Combustion Synthesis of Oxide Ceramic Powders", *Materials Letters*, September 1990 Volume 10, number 1, 2
- [9] R.D. Shannon, *Acta Cryst.*, 1976, pp. 751-767

This page intentionally left blank.

Distribution list

Document No.: DRDC Atlantic TM 2008-218

LIST PART 1: Internal Distribution by Centre

- 1 Author (G. Amow)
- 5 Library (1 hard copies, 4 CDs)

- 6 TOTAL LIST PART 1

LIST PART 2: External Distribution by DRDKIM

- 1 Library and Archives Canada, Attn: Military Archivist, Government Records Branch
- 1 NDHQ/DRDKIM

- 2 TOTAL LIST PART 2

8 TOTAL COPIES REQUIRED

This page intentionally left blank.

DOCUMENT CONTROL DATA

(Security classification of title, body of abstract and indexing annotation must be entered when the overall document is classified)

1. ORIGINATOR (The name and address of the organization preparing the document. Organizations for whom the document was prepared, e.g. Centre sponsoring a contractor's report, or tasking agency, are entered in section 8.) Defence R&D Canada – Atlantic 9 Grove Street P.O. Box 1012 Dartmouth, Nova Scotia B2Y 3Z7		2. SECURITY CLASSIFICATION (Overall security classification of the document including special warning terms if applicable.) UNCLASSIFIED	
3. TITLE (The complete document title as indicated on the title page. Its classification should be indicated by the appropriate abbreviation (S, C or U) in parentheses after the title.) Preliminary Study of the $\text{La}_{4-x}\text{A}_x\text{Ni}_3\text{O}_{10-\delta}$ (A = Na, K and Sr) Systems as IT-SOFC Cathode Materials (U)			
4. AUTHORS (last name, followed by initials – ranks, titles, etc. not to be used) Au, D.; Amow, G.			
5. DATE OF PUBLICATION (Month and year of publication of document.) May 2009	6a. NO. OF PAGES (Total containing information, including Annexes, Appendices, etc.) 32	6b. NO. OF REFS (Total cited in document.) 9	
7. DESCRIPTIVE NOTES (The category of the document, e.g. technical report, technical note or memorandum. If appropriate, enter the type of report, e.g. interim, progress, summary, annual or final. Give the inclusive dates when a specific reporting period is covered.) Technical Memorandum			
8. SPONSORING ACTIVITY (The name of the department project office or laboratory sponsoring the research and development – include address.) Defence R&D Canada – Atlantic 9 Grove Street P.O. Box 1012 Dartmouth, Nova Scotia B2Y 3Z7			
9a. PROJECT OR GRANT NO. (If appropriate, the applicable research and development project or grant number under which the document was written. Please specify whether project or grant.)		9b. CONTRACT NO. (If appropriate, the applicable number under which the document was written.)	
10a. ORIGINATOR'S DOCUMENT NUMBER (The official document number by which the document is identified by the originating activity. This number must be unique to this document.) DRDC Atlantic TM 2008-218		10b. OTHER DOCUMENT NO(s). (Any other numbers which may be assigned this document either by the originator or by the sponsor.)	
11. DOCUMENT AVAILABILITY (Any limitations on further dissemination of the document, other than those imposed by security classification.)			
12. DOCUMENT ANNOUNCEMENT (Any limitation to the bibliographic announcement of this document. This will normally correspond to the Document Availability (11). However, where further distribution (beyond the audience specified in (11) is possible, a wider announcement audience may be selected.)			

13. **ABSTRACT** (A brief and factual summary of the document. It may also appear elsewhere in the body of the document itself. It is highly desirable that the abstract of classified documents be unclassified. Each paragraph of the abstract shall begin with an indication of the security classification of the information in the paragraph (unless the document itself is unclassified) represented as (S), (C), (R), or (U). It is not necessary to include here abstracts in both official languages unless the text is bilingual.)

A preliminary study of the $\text{La}_{4-x}\text{A}_x\text{Ni}_3\text{O}_{10-\delta}$ (A = Na, K and Sr) system was carried out to determine their viability as IT-SOFC cathodes. For this study, two synthesis routes were used, both of which showed limited solubility ranges of the A-site doped cations. Physical property measurements show an enhancement of the electrical conductivity with A-site cation doping, good thermal stability and thermal expansion coefficients of $\alpha \sim 12.90 - 13.05 \times 10^{-6} \text{ K}^{-1}$. Scanning electron microscopy demonstrated significant differences in the particulate morphologies resulting from the different synthetic routes, which helps to explain the relatively rapid synthesis times of the glycine-nitrate process versus Pechini method.

14. **KEYWORDS, DESCRIPTORS or IDENTIFIERS** (Technically meaningful terms or short phrases that characterize a document and could be helpful in cataloguing the document. They should be selected so that no security classification is required. Identifiers, such as equipment model designation, trade name, military project code name, geographic location may also be included. If possible keywords should be selected from a published thesaurus, e.g. Thesaurus of Engineering and Scientific Terms (TEST) and that thesaurus identified. If it is not possible to select indexing terms which are Unclassified, the classification of each should be indicated as with the title.)

fuel cells; solid-oxide; Ruddlesden-Popper; cathodes

This page intentionally left blank.

Defence R&D Canada

Canada's leader in defence
and National Security
Science and Technology

R & D pour la défense Canada

Chef de file au Canada en matière
de science et de technologie pour
la défense et la sécurité nationale



www.drdc-rddc.gc.ca